Carbohydrate Polymers 114 (2014) 238–245

Contents lists available at ScienceDirect

Carbohydrate Polymers

journal homepage: www.elsevier.com/locate/carbpol

Nanostructured materials from hydroxyethyl cellulose for skin tissue engineering

Farah Hanani Zulkifli[a,*], Fathima Shahitha Jahir Hussain[a], Mohammad Syaiful Bahari Abdull Rasad[b], Mashitah Mohd Yusoff[a]

[a] Faculty of Industrial Sciences & Technology, University Malaysia Pahang, Lebuhraya Tun Razak, 26300 Gambang, Kuantan, Pahang, Malaysia
[b] Kulliyyah of Allied Health Sciences, International Islamic University Malaysia, Bandar Indera Mahkota Campus, Jalan Sultan Ahmad Shah, 25200 Kuantan, Pahang, Malaysia

ARTICLE INFO

Article history:
Received 27 January 2014
Received in revised form 13 August 2014
Accepted 14 August 2014
Available online 22 August 2014

Keywords:
Electrospinning
Hydroxyethyl cellulose
Nanofibrous scaffolds
Skin tissue engineering

ABSTRACT

In this study, a novel fibrous membrane of hydroxyethyl cellulose (HEC)/poly(vinyl alcohol) blend was successfully fabricated by electrospinning technique and characterized. The concentration of HEC (5%) with PVA (15%) was optimized, blended in different ratios (30–50%) and electrospun to get smooth nanofibers. Nanofibrous membranes were made water insoluble by chemically cross-linking by glutaraldehyde and used as scaffolds for the skin tissue engineering. The microstructure, morphology, mechanical and thermal properties of the blended HEC/PVA nanofibrous scaffolds were characterized by scanning electron microscope, Fourier transform infrared spectroscopy, differential scanning colorimetry, universal testing machine and thermogravimetric analysis. Cytotoxicity studies on these nanofibrous scaffolds were carried out using human melanoma cells by the MTT assays. The cells were able to attach and spread in the nanofibrous scaffolds as shown by the SEM images. These preliminary results show that these nanofibrous scaffolds that supports cell adhesion and proliferation is promising for skin tissue engineering.

1. Introduction

Research using nano-biomaterials as scaffold in skin tissue engineering is tremendously increasing as these biomaterials mimics the structure of extracellular matrix and provides a platform for cell attachment, differentiation and proliferation. The nanoscale biomaterials are produced by several methods including self-assembly, template assisted synthesis, drawing, phase separation and electrospinning (Kumbar, Nukavarapu, James, Nair, & Laurencin, 2008). However, electrospinning gains most interest among researchers because of the capability to fabricate a variety of polymeric nanofibers (Huang, Zhang, Kotaki, & Ramakrishna, 2003). Electrospinning is a technique that produces fibers in nanometer length and interconnected pores that closely resemble the topography features of ECM. It is a versatile technique to produce nano- and microfibers from polymer solutions or melts in the range of 30–200 nm, through the action of high electric field (Reneker & Chun, 1996; Taylor, Fang, & Reneker, 2006; Yarin, Koombhongse, & Reneker, 2001). When the electric field overcomes the surface tension, the polymer solution in the capillary is ejected as jets. The jets solidify as it travels toward the collector and is collected as nonwoven fabric. The morphology and properties of the nanofibers can be varied by changing the process parameters, such as solution viscosity and conductivity, applied voltage, average molecular weight of the polymer and the distance between the needle and the collector plate (Shin, Hohman, Brenner, & Rutledge, 2001; Zong et al., 2002; Zong, Ran, Fang, Hsiao, & Chu, 2003). The main attractions of the electrospun nanofibers are their unique properties such as high surface area-to-volume ratio, high porosity and their diameter, which is in the nanometer range.

Skin tissue engineering using scaffolds overcome the limitations from several wound healing processes like autografts, allografts and xenografts (Groeber, Holeiter, Hampel, Hinderer, & Schenke-Layland, 2011; Macneil, 2008). Scaffolds which have the suitable surface chemistry and excellent mechanical strength have been fabricated from several natural and synthetic polymers, which includes chitin, chitosan, polyurethane (PU), nylon, polyglycolic acid/polylactic acid (PGA/PLA), poly(L-lactide) (PLLA), polycaprolactone, and copolymer poly(ethyleneglycolterephthalate)-poly(butylenes terephthalate) (Beumer, van Blitterswijk, Bakker, & Ponec, 1993; Dai, Williamson, Khammo, Adams, & Coombes,

* Corresponding author. Tel.: +60 162054397.
E-mail address: fhanani01@yahoo.com (F.H. Zulkifli).

http://dx.doi.org/10.1016/j.carbpol.2014.08.019
0144-8617/

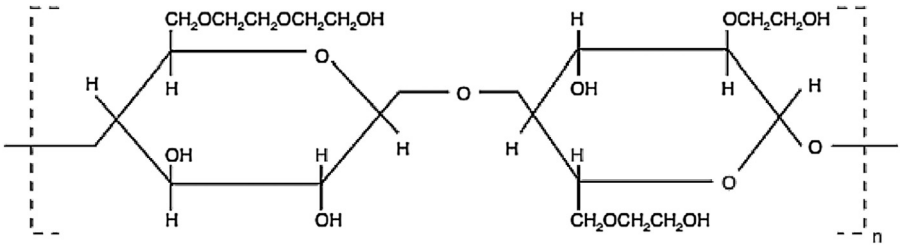

Fig. 1. Molecular structure of HEC.

2004). Fabrication of nanomaterials from most of these polymers require harmful or organic solvents or organic acid solvents like acrylic acid, acetic acid, chloroform, trifluoroacetic acid and 1,1,1,3,3,3-hexafluoro-2-propanol. In order to overcome the difficulties faced with the toxic solvents, in our research we have fabricated nanofibers, using water as the only solvent, from HEC and PVA. Moreover, the chemical structure of HEC exactly matches that of glycosaminoglycans (GAGs) in the dermis (Fig. 1); with specific GAGs of physiological significance are hyaluranic acid, dermatan sulfate and heparin. Although each of these GAGs has a predominant disaccharide component, heterogeneity does exist in the sugars present in the formation of any given class of GAG. HEC is a non-ionic hydrophilic polysaccharides biopolymers with β(1→4) glycosidic linkage. HEC groups attach to the OH groups of the polysaccharide structure by ether linkages. This hydrogel functions as a stabilizing and protective colloid. HEC is widely used in cosmetic, pharmaceutical and wound healing applications.

It is well known that these types of hydrogels with large amount of water diffused in three dimensional polymeric networks are highly needed in biomedical and health applications (Deligkaris, Tadele, Olthuis, & van den Berg, 2010). Cross-linking these hydrogels by various chemical bonds and physical interactions can significantly improve their mechanical, thermal and chemical properties (Mansur, Oréfice, & Mansur, 2004). Combination with other hydrogel like PVA, a biodegradable, non-toxic and non-carcinogenic hydrogel improves the spinnability and mechanical properties such as elasticity and elongation (Mansur & Mansur, 2007).

The main objective of this study is to develop biocompatible nanofibers from hydroxyethyl cellulose (HEC) together with the aqueous solution of PVA by electrospinning. The chemical and physical properties of the nanofibrous membrane from HEC/PVA were investigated after cross-linking it with glutaraldehyde. To the best of our knowledge, this is the first report where HEC is blended with PVA and electrospun to produce nanofibers and used as a scaffold material for skin tissue engineering. Studies on cell-scaffolds interaction was carried out by culturing human melanoma cells (A375) on these nanofibers and assessing the growth, proliferation and morphologies of the cells.

2. Materials and methods

2.1. Materials

Hydroxyethyl cellulose was purchased from Merck-Schumardt, Germany. Poly(vinyl alcohol) (molecular weight 95,000) was purchased from ACROS, New Jersey, USA. Analytical reagent grade glutaraldehyde was purchased from Merck-Schumardt, Germany, phosphoric acid was purchased from Merck.KGaA-Damstadt, Germany. Acetone was purchased from R&M Marketing, Essex, UK. Phosphate buffer saline (PBS) was purchased from Gibco Life Technologies, USA. All the chemicals were of highest purity and used without further purification. All the solutions were prepared using Milipore water.

2.2. Preparation of polymer solution

The HEC solution (5 wt%) was prepared by dissolving 5 g of HEC powder in 100 ml Millipore water and stirred for 2 h at room temperature until a clear solution was obtained with a slight increase in viscosity. PVA solution (15 wt%) was prepared by dissolving 15 g of PVA granules in 100 ml Millipore water with constant stirring at 80 °C for 2 h. For the blend solution, both HEC and PVA solutions were stirred continuously for 12 h at room temperature to ensure a complete mixing and eventually obtain a homogeneous solution. HEC was blended with PVA solution with three different weight ratios such as HEC:PVA, 50:50, 40:60 and 30:70.

2.3. Electrospinning of nanofibrous scaffolds

Electrospinning was carried out at room temperature for all the concentrations of HEC/PVA at a flow rate of 1 ml/h. The polymer solution was filled in a 5 ml syringe fitted with blunt steel needle of 0.8 mm inner diameter. The applied voltage was 25 kV. The electrospun nanofibers were collected using a rotating drum collector wrapped with aluminum foil with 12 cm of distance from tip-to-collector at a rotation speed of 1000 rpm. The humidity of 50% was preserved (Dri-Tech HT-180) in the room. The collected electrospun nanofibers were stored in desiccator for further use.

2.4. Cross-linking studies

The nanofibrous scaffolds were peeled and cut into 4 cm^2 pieces and kept in Petri dishes with diameter of 90 mm. Glutaraldehyde and acetone followed by phosphoric acid was added to the Petri dishes. This was kept aside for 24 h. Water resistance of the scaffolds was evaluated by immersing it in distilled water.

2.5. Characterization of nanofibrous scaffolds

2.5.1. Viscosity measurements

The viscosity of the electrospinning solutions was measures using Brookfield viscometer (Model DV-II + Pro). 20 ml of each blend solutions was taken in the built in stainless steel container of the viscometer and measurements were carried out at 25 °C.

2.5.2. Scanning electron microscopy (SEM) study

The surface morphology of HEC/PVA electrospun nanofibrous scaffolds before and after cross-linking was observed by a scanning electron microscopy (SEM) (ZEISS EVO 50) at an accelerating voltage of 15 kV. The electrospun nanofibers were sputter coated with a thin layer of platinum in double 30 s consecutive cycles at 45 mA to reduce charging and produce conductive surfaces (BALTEC SCD 005 Sputter Coater – BALTEC).

2.5.3. Attenuated total reflectance-Fourier transform infrared (ATR-FTIR) study

ATR-FTIR spectroscopic analysis of electrospun nanofibrous scaffolds was performed on Spectrum One (Perkin-Elmer, USA) spectrophotometer over a range of 500–4000 cm^{-1} at a resolution of 2 cm^{-1} with 100 scans per sample.

2.5.4. Differential scanning calorimeter (DSC) study

The thermal behavior of the electrospinning fibers was studied with a DSC technique. DSC was performed with a Q500 (TA Instruments, New Castle, USA) under nitrogen atmosphere. About 5 mg of sample was heat-treated from 50 to 250 °C at a heating rate of 10 °C/min. The degree of relative crystallinity, X_C was expected from the endothermic area by the following equation:

$$X_c = \frac{\Delta H_f}{\Delta H_f^\circ} \quad (1)$$

where ΔH_f = measured enthalpy of fusion from DSC thermograms and ΔH_f° = enthalpy of fusion for 100% crystalline PVA which is 138.6 J/g (Peppas & Merrill, 1976).

2.5.5. Thermogravimetric analysis (TGA) study

TGA was performed using Toledo STAR-1 (Mettler; Switzerland). About 5 mg of sample was heat treated from 30 to 750 °C at a heating rate of 10 °C/min under nitrogen atmosphere.

2.5.6. Mechanical testing

The mechanical properties of the electrospun nanofibers were measured using a universal testing machine (UTM) (AG-500, Shimadzu, Japan), under a cross-head speed of 10 mm/min. Rectangular specimens with dimension 10 mm × 20 mm were used for testing. The room conditions were controlled at 25 °C and 34% humidity. The tensile stress and strain at break were calculated based on the obtained tensile stress–strain curve.

2.6. Cell culture studies

2.6.1. Cell expansion and seeding

A375 cells were cultured in DMEM containing 10% FBS and 1% penicillin–streptomycin in 75 cm^2 cell culture flasks. The melanoma skin cells were incubated at 37 °C in a humidified atmosphere containing 5% CO_2 for 3 days. The cross-linked HEC/PVA (50:50) electrospun scaffolds were cut into small disks with 10 mm in diameter soaked in 100% ethanol for 24 h, and then sterilized under UV light for 3 h. These scaffolds were again sterilized with 70% ethanol for 30 min then washed with PBS for 15 min three times and subsequently immersed in cell culture medium overnight. The scaffolds were washed thrice with sterile PBS and transferred into 96-well tissue culture plate. A375 cells grown in 75 cm^2 cell culture flasks were detached on confluency by adding 1 ml of 0.25% trypsin containing 0.1% EDTA. Detached cells were centrifuged and counted by Trypan blue using hemocytometer, seeded on electrospun HEC/PVA nanofibrous scaffold at a density of 1×10^4 cells/cm^2 and incubated to facilitate cell growth. The medium was refreshed every 3 days.

2.6.2. Cell morphology studies

After 1, 4 and 7 days of cell culture, the A375 cells grown on scaffolds were rinsed twice with PBS and fixed in 3% glutaraldehyde for 30 min. Thereafter, the scaffolds were dehydrated with increasing concentrations of alcohol (20, 40, 60, 80 and 100%). The samples were air dried by keeping the samples in a fume hood. Lastly, the scaffolds were sputter coated with platinum and observed using SEM (ZEISS EVO 50) at an accelerating voltage of 10 kV.

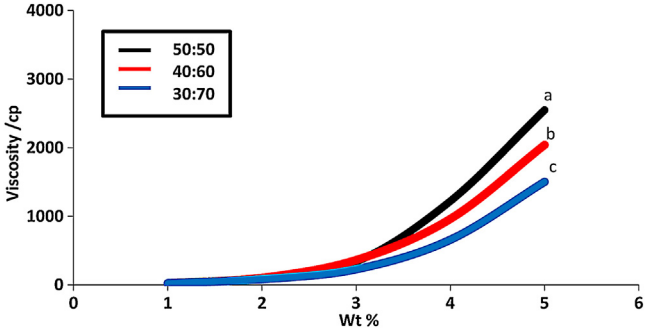

Fig. 2. Plot of the viscosity of the solution with respect to the wt% of the HEC/PVA (a) 50:50, (b) 40:60, (c) 30:70 in the solution.

2.6.3. Cell proliferation study

After certain time point, 10 μl of MTT solution (5 mg/ml) was added into the well plate and incubated at 37 °C for 4 h. The MTT solution was removed from each well and 100 μl of DMSO were added to each well to dissolve the MTT formazon crystals. The absorbance was recorded at 570 nm with background 630 nm by spectrophotometer. Since the absorbance at 570 nm is proportional to cell viability, the cell viability was calculating by following formula:

$$\text{Cell viabilty}\,(\%) = \frac{A_{\text{sample}}}{A_{\text{control}}} \times 100 \quad (2)$$

where A_{sample} = absorbance at 570 nm of the sample and $A_{control}$ = absorbance at 570 nm of the positive control which is cells in complete medium incubated in the absence of the scaffolds. Each experiment was performed in triplicate.

3. Results and discussion

3.1. Morphology of HEC/PVA nanofibrous membranes

Viscosity is one of the important parameters in the spinning process of nanofibers. The solution viscosity of HEC (5 wt%) was 2555 cp and that of PVA (15 wt%) was 395 cp. With the increase in the amount of HEC in the HEC/PVA blend from 30% to 50%, the viscosity of the solution was increased significantly from 1504 cp to 2550 cp (Fig. 2). Although the viscosity of HEC is high, nanofibers from HEC were difficult to obtain (Fig. 3). It is because properties of the polymer solution such as surface tension, electrical conductivity and polymer concentrations influence the electrospinning process (Huang et al., 2003). With concentration lower than 5 wt%,

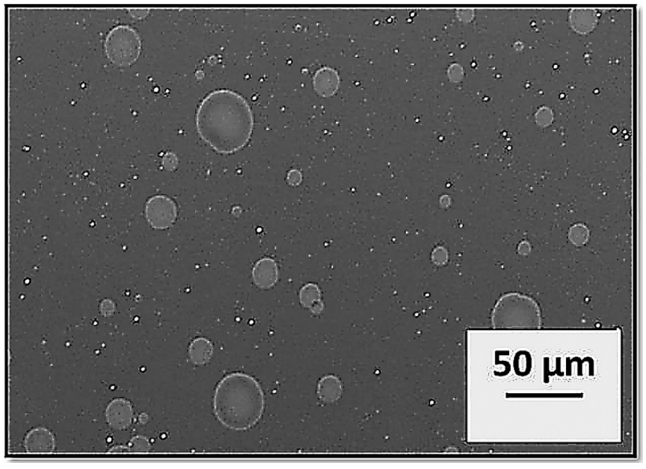

Fig. 3. SEM images of HEC nanofibers.

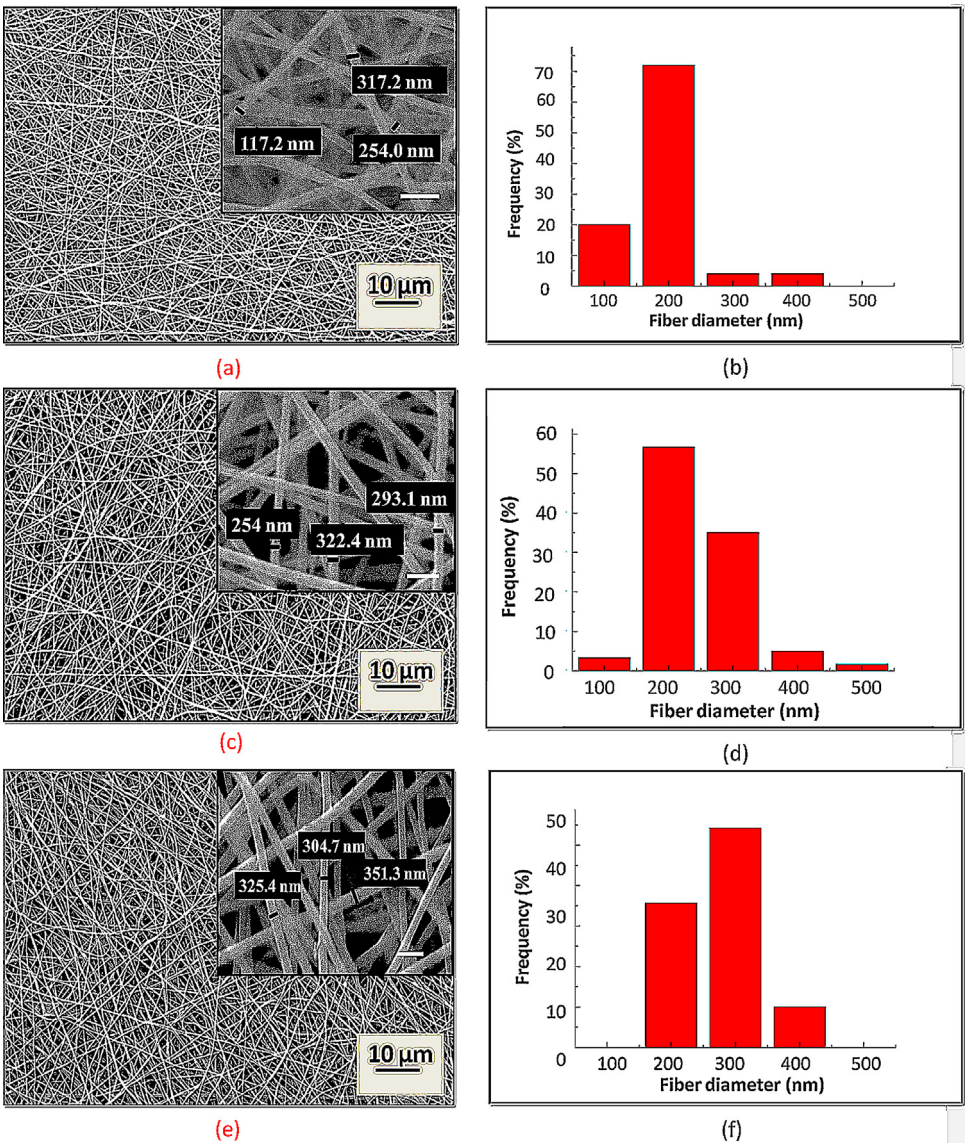

Fig. 4. SEM images and diameter distribution of electrospun HEC/PVA nanofibers with different weight ratios of HEC to PVA: (a, b) 50:50, (c, d) 40:60, (e, f) 30:70. Inert scale bars: 1 μm.

drops were formed and with high concentration >5 wt%, the flow of solution out of the needle is low. Fig. 4 shows the SEM images of nanofibrous scaffolds at different weight ratios of HEC/PVA: 50:50, 40:60 and 30:70 and their corresponding diameter distribution. The images revealed uniform, porous, beadless and nano-scaled fibrous structures formed under control condition (Table 1). Fiber diameters were in the ranges of 241.90 ± 17.03 nm, 292.95 ± 25.06 nm and 320 ± 27.17 nm for 50:50, 40:60 and 30:70 of HEC/PVA respectively. This is comparable to the diameter of dermal collagen fibrils of native human skins which in the range of 60–70 nm (Wang & Carrier, 2011) and ~300 nm long-fibrils (Kühn, 1987). The morphological similarity of electrospun nanofibers to native ECM; consists of various interwoven protein fibers with diameters ranging from tens to hundreds of nanometer, signifies the application of these scaffolds as a supportive matrix for stem cell attachment and differentiations (Prabhakaran, 2012). Nanofibers scaffolds that mimic the fibrous ECM molecules in the native skins could provide mechanical, biological and chemical cues to the cells for tissue

Table 1
Electrospinning parameters for HEC/PVA nanofibers and their corresponding average fiber diameter.

Sample code	Electrospinning parameters					
	HEC/PVA ratio	Rotation speed (rpm)	Tips-to-collector distance (mm)	Flow rate (ml/h)	Applied voltage (kV)	Average fiber diameter (nm)
HEC/PVA (50:50)	50:50	1000	110	1	20	241.90 ± 17.03
HEC/PVA (40:60)	40:60	1000	100	1	20	292.95 ± 25.06
HEC/PVA (30:70)	30:70	1000	90	1	20	320 ± 27.17

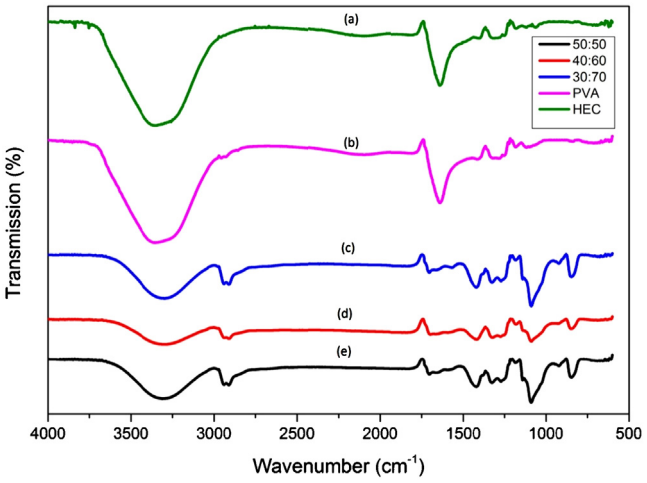

Fig. 5. FTIR spectra for (a) HEC, (b) PVA, nanofibers at different weight ratio of HEC to PVA (c) 50:50, (d) 40:60 and (e) 30:70.

morphogenesis, differentiation and homeostasis (Frantz, Stewart, & Weaver, 2010). By electrospinning, it was hard to get fibers for HEC alone. Therefore, PVA was blended with HEC to enhance the fiber formation efficiency. The time required for blending the two polymers plays an important role. The polymers have to be stirred for at least 12 h to get good fibers. A significant increase in fiber diameter with the increase of PVA composition was observed. The nanofiber diameter increased sharply and the diameter distribution became lesser with the increase of PVA concentration. Similar result was obtained by Shalumon et al. (2009) showing that the increase in the amount of PVA in mixed solution will produce fine nanofibers with increasing fiber diameters. However, fiber formation distribution was found to be decreasing when PVA amounts was increased in blended solution.

3.2. ATR-FTIR study

FTIR spectroscopy was carried out to elucidate the presence of HEC and PVA in the blended nanocomposite and to analyze the interaction (hydrogen bonding) between them. The FTIR transmission spectra of pure HEC and PVA solution and HEC/PVA nanofiber are shown in Fig. 5. The results indicate that the incorporation of HEC into PVA nanofibers causes increasing in crystallinity which was clearly evidences by strengthening of the crystalline band at 1143 cm^{-1}. The strong peaks observed from 759 to 937 cm^{-1} exhibited the C—H and CH_2 bending vibrations while the high peak at 1711 cm^{-1} corresponding to the CO stretching exists in both HEC and PVA solution was completely missing in the electrospun fibers of HEC/PVA nanocomposite nanofibers. It is also observed that the absorption bands associated with OH stretching appeared at 3278 cm^{-1} in the spectrum of HEC and PVA is highly reduced in its intensity for HEC/PVA electrospun nanofibers. This might be due to the loose physisorbed water at the surface of collected fibers during the electrospinning process. However, this strong intermolecular hydrogen bonding between the molecules in the electrospun HEC/PVA nanofibers was clearly due to the presence of large number of OH groups (Zhang, Nie, Li, White, & Zhu, 2009).

3.3. TGA measurements

The TGA and DrTGA of all samples are illustrated in Fig. 6(a)–(c). The TGA thermograms for electrospun nanofibers exhibited three major weight loss stages which is ~5 wt% at 3–260 °C. This low value of percentage mass loss is due to the weakly physisorbed water or weak evaporation of bound water. The latter process in

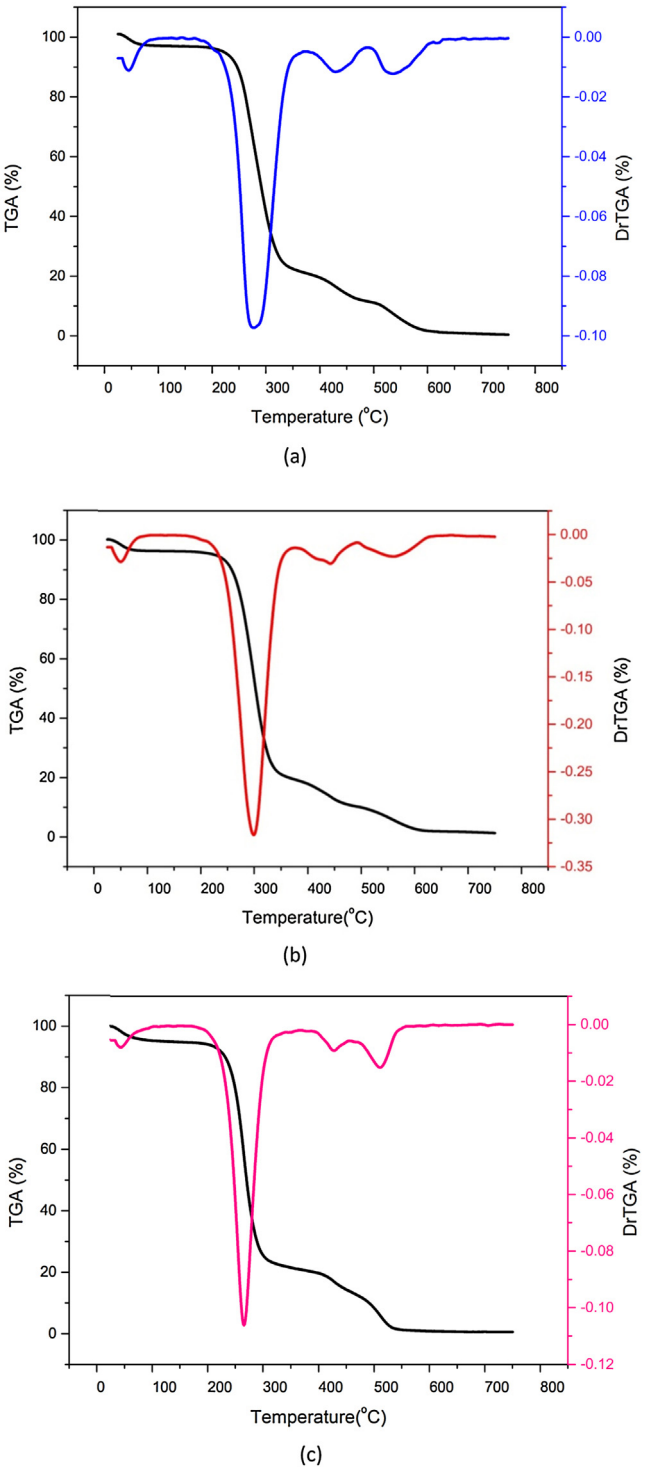

Fig. 6. (a–c) TGA and DrTGA curves for electrospun nanofibers at weight ratio of HEC to PVA: (a) 50:50, (b) 40:60, (c) 30:70.

TGA curves covers the melting point of PVA and the thermal degradation of the samples. The decomposition of side chain of PVA occurs at in the range of 260–400 °C which contributed to ~75% of the mass loss in second decomposition stage is also due to the loss of CO_2, in the concern of HEC. The decomposition of main chain of PVA occurs at 400–540 °C. It is observed that the peak temperature of elecrospun nanofibers is shifted to higher temperatures with increasing of HEC contents. This indicated that the HEC is more

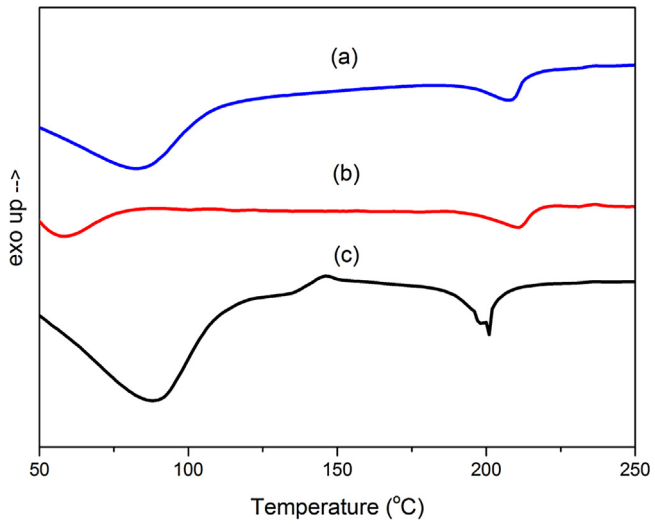

Fig. 7. DSC thermograms for nanofibers at different weight ratio of HEC to PVA (a) 50:50, (b) 40:60 and (c) 30:70.

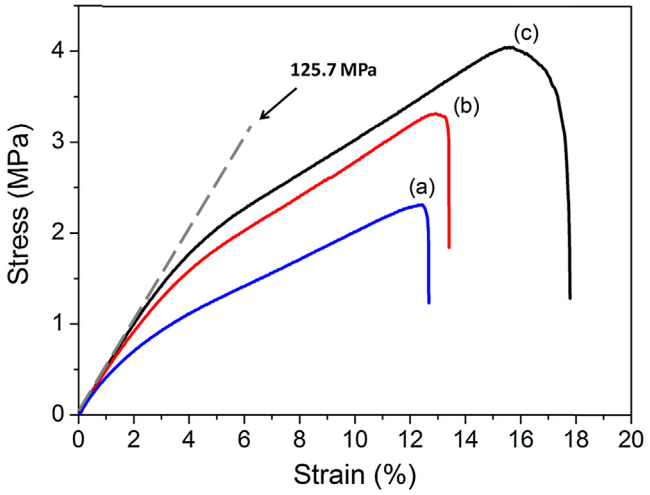

Fig. 8. Stress–strain curves for nanofibers at different weight ratio of HEC to PVA (a) 50:50, (b) 40:60 and (c) 30:70.

stable than PVA where the chemical structure plays an important role in the thermal decomposition process.

3.4. DSC study

DSC measurement has been done to investigate the thermal behavior of electrospun nanofibers such as melting (T_m), crystallization (T_c) and glass transition (T_g) phenomena. The results from DSC and the characterization observed for electrospun nanofibers are shown in Fig. 7 and characterized in Table 2.

DSC thermograms show characterization by a change in heat capacity of the mats associated with endothermic glass transition of PVA at 96.11 °C, 58.19 °C and 70.02 °C and followed by single melting peak resulting from a partial crystallization at 208.05 °C, 210.96 °C and 200.57 °C for sample 50:50, 40:60 and 30:70 respectively. The broad glass transition peak may be due to the overlapping transitions of two polymer blend samples (Shalumon et al., 2009). This endotherm is attributed to the liberation of absorbed moisture and not the melting point of HEC. The enthalpy that is associated with endotherm melting transition of electrospun nanofibers was found to be higher with increasing PVA content, with the peak position remaining approximately unaltered. It is well known that PVA has a sharp endothermic curve with a peak at 200 °C. This increment could be attributed to the segmental motions of polymer chains which were greatly constricted by the strong interactions between them through hydrogen bonds. It is well known that that the heat required for 100% melting PVA is 138.6 J/g (Peppas & Merrill, 1976). Therefore, the relatively weak and broadened glass transitions can be ascribed to the semicrystalline nature of the material. By calculating the degree of crystallinity, X_c it is found that the X_C is decreased with the reduced amount of PVA content. This decrement is attributed to the strong hydrogen bonds with the hydroxyl group which indicate the compatibility between HEC and PVA (Asran, Henning, & Michler, 2010) and shows that HEC reduces the crystallinity of the blend nanofibers.

Table 2
DSC data and the characteristics observed for the electrospun nanofibers.

Sample (HEC:PVA)	T_g (°C)	T_m (°C)	ΔH_m (J/g)	Crystallinity (%)
50:50	96.11	208.05	18.71	13.50
40:60	58.19	210.96	35.58	25.67
30:70	70.02	200.57	37.16	26.81

3.5. Mechanical characterization

Mechanical properties such as tensile strength and elongation at break of different nanofibrous scaffolds were evaluated during this study. Typical nonlinear stress–strain curves of electrospun scaffolds at different ratio are shown in Fig. 8. The calculated Young's modulus based on slope shown in the elastic region was measured and found to be approximately 125.7 MPa. This is comparable to the tensile modulus of human skin which lies in the range of 15–150 MPa (Edwards & Marks, 1995). The stress at breakage was found to be 2.31 MPa, 3.3 MPa and 4.04 MPa, with elongation at break of 12.4%, 13.2% and 15.7% for sample 50:50, 40:60 and 30:70 respectively. Higher tensile stress and strain values were obtained with the increasing of PVA value. The ultimate tensile stress (MPa) and strain (%) value of blended nanofibrous scaffold is low compared with that of human skin which is in range 5–30 MPa and 35–115% respectively (Edwards & Marks, 1995). However, previous report found that tensile strength of electrospun fiber mats ranging from 0.8 to 18.0 MPa was sufficiently durable for dermal cell culture (Barnes, Sell, Boland, Simpson, & Bowlin, 2007; He, Ma, Yong, Teo, & Ramakrishna, 2005). In addition, fibrous scaffolds as potential skin graft is seldom under a high tensile strength when immobilized at a wound site and it is not necessary for the scaffolds to be permanent replacement for native tissue and replicate the host environment (Cui, Zhu, Yang, Li, & Jin, 2009; Jin, Prabhakaran, & Ramakrishna, 2011). So, these scaffolds are mechanically stable and could serve as a temporary constructs for skin tissue engineering.

3.6. Cell scaffold interaction study

3.6.1. Cell morphology study of A375 cells

Fig. 9 shows the morphology of human A375 melanoma cells on different scaffolds on days 3 and 7 observed by SEM. Seeded A375 cells were adhered and had spread well on the scaffolds in a time depended manner. It was observed that at 3 days time point, the cells started to adhere and spread at the surface of nanofibers in a flat morphology. The attached cells become rounded and appeared in globular morphology on the scaffolds after day 7 (Mei et al., 2012). In addition, it was observed that there was a greater tendency of cell spreading with increased of PVA contents. These cells were growth with effective spreading, indicating that scaffolds exhibited excellent biocompatibility.

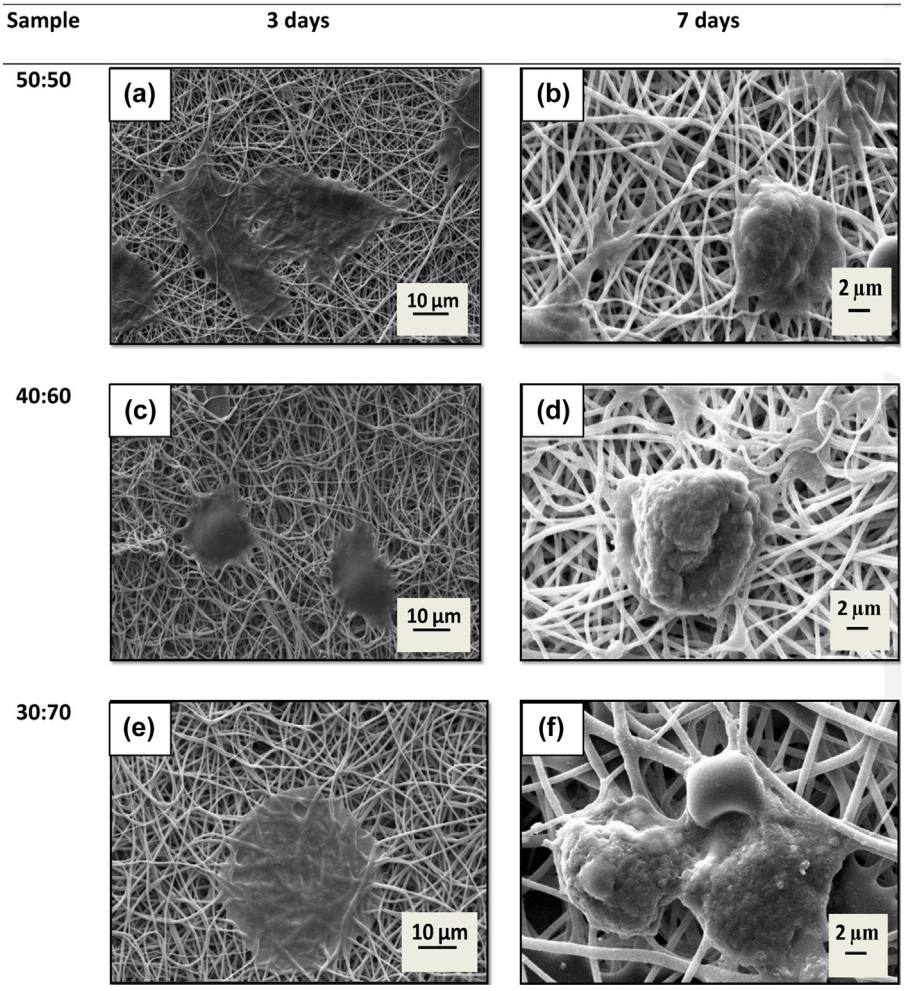

Fig. 9. SEM micrographs of human A375 melanoma cells attached on nanofibrous scaffolds at different weight ratios of HEC to PVA: (a, b) 50:50, (c, d) 40:60 and (e, f) 30:70.

3.6.2. Cell proliferation on HEC/PVA nanofibrous scaffolds

The proliferation of human A375 melanoma cells on the nanofibrous scaffolds was studied by examining cell viability on days 1, 3 and 7. By using cells in a complete media without the presences of scaffold as a positive control, the relative cell viability on each scaffold was calculated and exemplified in Fig. 10. As shown in Fig. 10, all nanofibrous scaffolds showed significant increases ($p \leq 0.05$) from day 1 to day 7 due to the increase number of cell attachment and penetration through the porous fibers. These increments are due to less hydrophobic surfaces of the HEC/PVA nanofibrous scaffolds which enhance the cells growth. The percentage of cell viability from day 1 to day 3 showed augmentation up to ~70% compared to cell viability from day 3 to day 7 which is only up to ~25%. This indicated an excellent initial adhesion between cells and randomly oriented nanofibrous scaffolds.

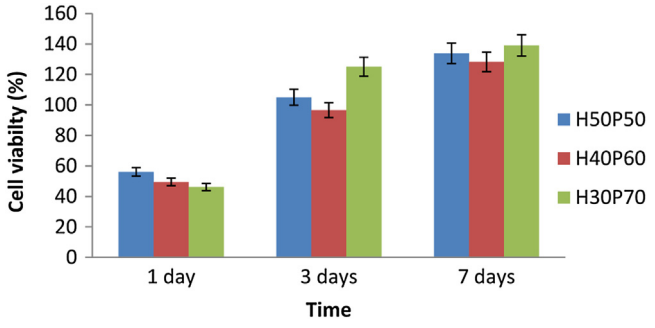

Fig. 10. Graph showing human A375 melanoma viability after 1, 3 and 7 days of incubation (1×10^4 cells/well in complete DMEM) at different weight ratios of nanofibrous scaffolds. (H – HEC content; P – PVA content)

4. Conclusion

In this study, HEC/PVA as a water soluble biocompatible polymer was successfully electrospun as nanofibers. The fibrous mats were cross-linked with glutaraldehyde to get water insoluble nanofibrous scaffolds. The effect of different weight ratios of HEC/PVA solutions on nanofiber formation, morphology, mechanical, thermal and stability of HEC/PVA fibers was studied. The HEC/PVA nanofibrous scaffolds exhibited good biocompatibility. The scaffolds showed enhanced cell viability with increasing culture time. Hence, these biocompatible and biodegradable scaffolds are promising materials for tissue engineering applications.

Acknowledgements

This work was supported by the Fundamental Research Grant Scheme (FRGS) RDU100106. The authors acknowledge the support from the Faculty of Industrial Science and Technology at the Universiti Malaysia Pahang.

References

Asran, A. S., Henning, S., & Michler, G. H. (2010). Polyvinyl alcohol-collagen-hydroxyapatite biocomposite nanofibrous scaffold: Mimicking the key features of natural bone at the nanoscale level. *Polymer*, *51*(4), 868–876. http://dx.doi.org/10.1016/j.polymer.2009.12.046

Barnes, C. P., Sell, S. A., Boland, E. D., Simpson, D. G., & Bowlin, G. L. (2007). Nanofiber technology: Designing the next generation of tissue engineering scaffolds. *Advanced Drug Delivery Reviews*, *59*(14), 1413–1433. http://dx.doi.org/10.1016/j.addr.2007.04.022

Beumer, G. J., van Blitterswijk, C. A., Bakker, D., & Ponec, M. (1993). Cell-seeding and in vitro biocompatibility evaluation of polymeric matrices of PEO/PBT copolymers and PLLA. *Biomaterials*, *14*(8), 598–604. Retrieved from http://www.sciencedirect.com/science/article/pii/0142961293901785

Cui, W., Zhu, X., Yang, Y., Li, X., & Jin, Y. (2009). Evaluation of electrospun fibrous scaffolds of poly(DL-lactide) and poly(ethylene glycol) for skin tissue engineering. *Materials Science and Engineering C*, *29*(6), 1869–1876. http://dx.doi.org/10.1016/j.msec.2009.02.013

Dai, N.-T., Williamson, M. R., Khammo, N., Adams, E. F., & Coombes, a. G. a. (2004). Composite cell support membranes based on collagen and polycaprolactone for tissue engineering of skin. *Biomaterials*, *25*(18), 4263–4271. http://dx.doi.org/10.1016/j.biomaterials.2003.11.022

Deligkaris, K., Tadele, T. S., Olthuis, W., & van den Berg, A. (2010). Hydrogel-based devices for biomedical applications. *Sensors and Actuators B: Chemical*, *147*(2), 765–774. http://dx.doi.org/10.1016/j.snb.2010.03.083

Edwards, C., & Marks, R. (1995). Evaluation of biomechanical properties of human skin. *Clinics in Dermatology*, *13*, 375–380. Retrieved from http://courses.washington.edu/bioen327/Labs/Lit_BiomechPropsSkin.pdf

Frantz, C., Stewart, K. M., & Weaver, V. M. (2010). The extracellular matrix at a glance. *Journal of Cell Science*, *123*(Pt 24), 4195–4200. http://dx.doi.org/10.1242/jcs.023820

Groeber, F., Holeiter, M., Hampel, M., Hinderer, S., & Schenke-Layland, K. (2011). Skin tissue engineering—In vivo and in vitro applications. *Advanced Drug Delivery Reviews*, *63*(4–5), 352–366. http://dx.doi.org/10.1016/j.addr.2011.01.005

He, W., Ma, Z., Yong, T., Teo, W. E., & Ramakrishna, S. (2005). Fabrication of collagen-coated biodegradable polymer nanofiber mesh and its potential for endothelial cells growth. *Biomaterials*, *26*(36), 7606–7615. http://dx.doi.org/10.1016/j.biomaterials.2005.05.049

Huang, Z.-M., Zhang, Y.-Z., Kotaki, M., & Ramakrishna, S. (2003). A review on polymer nanofibers by electrospinning and their applications in nanocomposites. *Composites Science and Technology*, *63*(15), 2223–2253. http://dx.doi.org/10.1016/S0266-3538(03)00178-7

Jin, G., Prabhakaran, M. P., & Ramakrishna, S. (2011). Stem cell differentiation to epidermal lineages on electrospun nanofibrous substrates for skin tissue engineering. *Acta Biomaterialia*, *7*(8), 3113–3122. http://dx.doi.org/10.1016/j.actbio.2011.04.017

Kühn, K. (1987). The classical collagens: Types I, II, and III. In R. Saynes (Ed.), *Structure and function of collagen types* (pp. 1–42). Academic Press. http://dx.doi.org/10.1016/B978-0-12-481280-2.50005-2

Kumbar, S. G., Nukavarapu, S. P., James, R., Nair, L. S., & Laurencin, C. T. (2008). Electrospun poly(lactic acid-co-glycolic acid) scaffolds for skin tissue engineering. *Biomaterials*, *29*(30), 4100–4107. http://dx.doi.org/10.1016/j.biomaterials.2008.06.028

Macneil, S. (2008). *Biomaterials for tissue engineering of skin*, *11*(5), 26–35.

Mansur, H. S., & Mansur, A. A. P. (2007). *Synchrotron SAXS, XRD and FTIR characterization of nanostructured PVA/TEOS hybrid cross-linked with glutaraldehyde*. *Diffusion and defect data Pt. B: Solid state phenomena* (vols. 121–123). Retrieved from http://www.scopus.com/inward/record.url?eid=2-s2.0-385491609978&partnerID=tZOtx3y1

Mansur, H. S., Oréfice, R. L., & Mansur, A. A. P. (2004). Characterization of poly(vinyl alcohol)/poly(ethylene glycol) hydrogels and PVA-derived hybrids by small-angle X-ray scattering and FTIR spectroscopy. *Polymer*, *45*(21), 7193–7202. Retrieved from http://www.sciencedirect.com/science/article/pii/S0032386104008109

Mei, L., Hu, D., Ma, J., Wang, X., Yang, Y., & Liu, J. (2012). Preparation, characterization and evaluation of chitosan macroporous for potential application in skin tissue engineering. *International Journal of Biological Macromolecules*, *51*(5), 992–997. http://dx.doi.org/10.1016/j.ijbiomac.2012.08.004

Peppas, N. A., & Merrill, E. W. (1976). Differential scanning calorimetry of crystallized PVA hydrogels. *Journal of Applied Polymer Science*, *20*(6), 1457–1465. http://dx.doi.org/10.1002/app.1976.070200604

Prabhakaran, M. P. (2012). Stem cells and nanostructures for advanced tissue regeneration. In R. Jayakumar, & S. Nair (Eds.), *Biomedical applications of polymeric nanofibers* (pp. 21–58). Springer Science & Business Media. Retrieved from http://books.google.com/books?id=WINYlWPM8FgC&pgis=1

Reneker, D. H., & Chun, I. (1996). Nanometre diameter fibres of polymer, produced by electrospinning. *Nanotechnology*, *7*(3), 216–223. http://dx.doi.org/10.1088/0957-4484/7/3/009

Shalumon, K. T., Binulal, N. S., Selvamurugan, N., Nair, S. V., Menon, D., Furuike, T., et al. (2009). Electrospinning of carboxymethyl chitin/poly(vinyl alcohol) nanofibrous scaffolds for tissue engineering applications. *Carbohydrate Polymers*, *77*(4), 863–869. http://dx.doi.org/10.1016/j.carbpol.2009.03.009

Shin, Y. M., Hohman, M. M., Brenner, M. P., & Rutledge, G. C. (2001). Experimental characterization of electrospinning: The electrically forced jet and instabilities. *Polymer*, *42*(25), 09955–09967. http://dx.doi.org/10.1016/S0032-3861(01)00540-7

Taylor, P., Fang, X., & Reneker, D. H. (2006). DNA fibers by electrospinning. *Journal of Macromolecular Science, Part B: Physics*, (December 2013), 37–41.

Wang, L. L., & Carrier, R. (2011). Biomimetic topography: Bioinspired cell culture substrates and scaffolds. In A. George (Ed.), *Advances in biomimetics* (pp. 433–472). InTech. http://dx.doi.org/10.5772/574

Yarin, A. L., Koombhongse, S., & Reneker, D. H. (2001). Bending instability in electrospinning of nanofibers. *Journal of Applied Physics*, *89*(5), 3018. http://dx.doi.org/10.1063/1.1333035

Zhang, H., Nie, H., Li, S., White, C. J. B., & Zhu, L. (2009). Crosslinking of electrospun polyacrylonitrile/hydroxyethyl cellulose composite nanofibers. *Materials Letters*, *63*(13–14), 1199–1202. http://dx.doi.org/10.1016/j.matlet.2009.02.035

Zong, X., Kim, K., Fang, D., Ran, S., Hsiao, B. S., & Chu, B. (2002). Structure and process relationship of electrospun bioabsorbable nanofiber membranes. *Polymer*, *43*(16), 4403–4412. http://dx.doi.org/10.1016/S0032-3861(02)00275-6

Zong, X., Ran, S., Fang, D., Hsiao, B. S., & Chu, B. (2003). Control of structure, morphology and property in electrospun poly(glycolide-co-lactide) non-woven membranes via post-draw treatments. *Polymer*, *44*(17), 4959–4967. http://dx.doi.org/10.1016/S0032-3861(03)00464-6